reactions

MDPI

Article

Regioselective Bond-Forming and Hydrolysis Reactions of Doubly Charged Vanadium Oxide Anions in the Gas Phase

Chiara Salvitti *, Federico Pepi, Anna Troiani * and Giulia de Petris

Dipartimento di Chimica e Tecnologie del Farmaco, "Sapienza" University of Rome, P.le Aldo Moro 5, 00185 Rome, Italy; federico.pepi@uniroma1.it (F.P.); giulia.depetris@uniroma1.it (G.d.P.)
* Correspondence: chiara.salvitti@uniroma1.it (C.S.); anna.troiani@uniroma1.it (A.T.)

Abstract: The gas-phase reactivity of vanadium-containing dianions, $NaV_3O_9^{2-}$ and its hydrated form $H_2NaV_3O_{10}^{2-}$, were probed towards sulphur dioxide at room temperature by ion-molecule reaction (IMR) experiments in the collision cell of an ion trap mass spectrometer. The sequential addition of two SO_2 molecules to the $NaV_3O_9^{2-}$ dianion leads to the breakage of the stable V_3O_9 backbone, resulting in a charge separation process with the formation of new V-O and S-O bonds. On the contrary, the $H_2NaV_3O_{10}^{2-}$ hydroxide species reacts with SO_2, promoting regioselective hydrolysis and bond-forming processes, the latter similar to that observed for the $NaV_3O_9^{2-}$ reactant anion. Kinetic analysis shows that these reactions are fast and efficient with rate constants of the 10^{-9} ($\pm$30) $cm^3\ s^{-1}$ $molecule^{-1}$ order of magnitude.

Keywords: vanadium oxide reactivity; sulphur dioxide; mass spectrometry; ion-molecule reactions; bond-forming reactions; hydrolysis reactions

Citation: Salvitti, C.; Pepi, F.; Troiani, A.; de Petris, G. Regioselective Bond-Forming and Hydrolysis Reactions of Doubly Charged Vanadium Oxide Anions in the Gas Phase. *Reactions* **2022**, *3*, 254–264. https://doi.org/10.3390/reactions3020019

Academic Editor: Dmitry Yu. Murzin

Received: 28 February 2022
Accepted: 1 April 2022
Published: 5 April 2022

1. Introduction

Vanadium-based compounds find several applications in a wide range of research fields. For example, supported vanadium oxides are largely employed in the metallurgic industry as heterogeneous catalysts for the manufacture of important chemicals [1]. Among these, sulphuric acid is considered an excellent indicator of the "industrial strength" of a nation, being one of the most produced chemicals worldwide [2]. More recently, vanadium hydroxides have also attracted interest as secondary electrode materials in the design of Li-ion and redox flow batteries [3–6].

Considering the significant potential of vanadium species, the chemical features of these compounds have been extensively investigated both in the solution and in the gas-phase environments. The latter represents a designable arena in which a variety of different experiments performed by means of mass spectrometric techniques allow one to elucidate structural and thermochemical features of ionic clusters. The refined control of the cluster size, charge, and stoichiometry in the absence of perturbing effects can indeed contribute to assessing the elementary steps of a complex process at a strictly molecular level, obtaining detailed mechanistic information [7–13]. Accordingly, the reactivity of vanadium oxide mono-cations and anions was probed towards selected hydrocarbons, water, and SO_2 by ion-molecule reaction (IMR) experiments [14–31]. In particular, it has been reported that the vanadium-oxide kernel of the $V_4O_{10}^-$ anion can effectively incorporate SO_2, leading to a $[V_4O_{10}\text{-}SO_2]^-$ complex with a square pyramidal structure [29], whereas neutral vanadium oxides only give association intermediates or oxidation and reduction products by the reaction with SO_2 [32,33].

Although many studies in the literature describe the gas-phase reactivity of mono-charged vanadium oxide ions, the chemistry of the corresponding multi-charged species has been only partially explored. These ions can be generated by electrospray ionization (ESI) processes by the direct transfer of charged species formed in solution under mild

conditions into the gas-phase environment [34]. In particular, we refer both to small doubly-charged species (e.g., VO^{2+}, VOH^{2+}, VOH^{2+}) stabilized as water adducts [35] and large multiply-charged polyoxovanadates in which vanadium can assume different oxidation states and a variety of intriguing geometries [36].

The typical gas-phase reactions of dications are the so-called bond-forming processes where the simultaneous breakage and formation of chemical bonds lead to two singly-charged ions and/or a new doubly-charged species [37–44]. On the contrary, dianions are commonly involved in proton-transfer and substitution/elimination reactions always resulting in the incorporation of the intact dianion in the final product scaffold [45–47]. Recently, we reported the unprecedented bond-forming reactivity of doubly-charged vanadium hydroxoanions in the gas phase studied by IMR experiments and theoretical calculations [48,49]. $H_2V_2O_7^{2-}$ and $HNaV_4O_{12}^{2-}$ react with SO_2, leading to $H_2VO_4^-$ and $VO_3SO_2^-$, and to $NaV_4O_{11}^-$ and $HOSO_2^-$, respectively [48]. These singly-charged products are formed through the action of SO_2, which effectively favors the breakage of the stable V_2O_7 kernel of $H_2V_2O_7^{2-}$ and the terminal V-OH bond of $HNaV_4O_{12}^{2-}$ dianions. Furthermore, a cooperative effect was evidenced in complexes of the $V_2O_6^{2-}$ and $HV_3O_{10}^{2-}$ formula with SO_2 in favoring a hydrolysis reaction, giving rise to the charge separation of the dianion along with the formation of the $HOSO_2^-$ bisulfite anion [49].

Continuing with our studies focused on the gas-phase activation of SO_2 [50–56], here we report on the reactivity of two polyoxovanadate dianions, namely $NaV_3O_9^{2-}$ and $H_2NaV_3O_{10}^{2-}$, towards SO_2 by using IMR mass spectrometry. The reactions are very fast and efficient and lead to singly charged products that do not contain the reactants in the molecular scaffold. Cooperative effects and regioselectivity were demonstrated when addressing different reaction outcomes, providing new interesting examples of bond-forming and hydrolysis reactions in the gas phase.

2. Materials and Methods

2.1. Materials

The research-grade chemicals and solvents employed in this study were purchased from Sigma-Aldrich and used without further purification. The stated purities of the chemicals, as reported by the vendor, are as follows: $NaVO_3$ (99.9%), SO_2 (99.9%), whereas H_2O and CH_3CN solvents are at the HPLC grade.

Pure N_2 (99.995%) and He (99.995%) gases were purchased from Nippon Gases.

2.2. Mass Spectrometry

All the experiments were carried out on an LTQ XL linear ion trap mass spectrometer (Thermo Fisher Scientific, Bremen, Germany) that was in-house modified to perform ion-molecule reactions and study the kinetic profiles of gas-phase processes [57]. The instrument was equipped with an electrospray ionization (ESI) source operating in negative ion mode, under the following experimental conditions: source voltage of 2–3 kV and capillary temperature of 275 °C. Nitrogen (N_2) was used as sheath and auxiliary gas at a flow rate of 3.7 and 0.74 L min^{-1}, respectively [58]. Capillary and tube lens voltages were set to low values (in the range of −1 and −10 V) to maximize the formation of multiply-charged ions at the expense of singly-charged species [48,49].

Millimolar solutions of $NaVO_3$ in H_2O/CH_3CN (1/3 *v/v)* were infused into the ESI source via the on-board syringe pump at a flow rate of 5 μL min^{-1}, whereas neutral sulphur dioxide (SO_2) was separately introduced into the ion trap through a deactivated fused-silica capillary that entered the vacuum chamber from a 6.25 mm hole placed in the backside of the mass spectrometer. The pressure of the neutral gas was kept constant by a metering valve and measured by a Granville−Phillips Series 370 Stabil Ion Vacuum Gauge. Owing to the position of the Pirani gauge, the actual SO_2 pressure was estimated based on a calibration of the pressure reading [59]. Typical pressures of SO_2 ranged between 1.1×10^{-7} and 7.6×10^{-7} Torr.

The $NaV_3O_9^{2-}$ and $H_2NaV_3O_{10}^{2-}$ reactant ions were generated in the ESI source and thermalized by collisions with background helium during the transfer and inside the trap (collision frequency $\approx 10^5 \cdot s^{-1}$). After 0.1–0.2 s, they were mass-to-charge isolated and reacted with SO_2. The signals of the ionic reactant and products were monitored over time as a function of the SO_2 concentration, and for each reaction time an average of 10 scan acquisitions were acquired. The normalized collision energy was set to zero, and the activation *Q* value was optimized to ensure stable trapping fields for all the ions under investigation.

To measure the rate constants, logarithmic plots of the reactant species concentration vs. time were constructed. Accordingly, all the studied reactions display a pseudo-first-order decay. Experimental data obtained from the kinetic analysis were fitted to a mathematical model built on the basis of the hypothesized reaction mechanism by using Dynafit 4 package [60]. Bimolecular rate constants *k* (cm^3 $molecule^{-1}$ s^{-1}) were derived as a product of the pseudo-first-order constants (s^{-1}) divided by the concentration of neutral reagent gas. To ensure the accuracy of the *k* values, ca. 10–15 independent measurements for each precursor ion were performed on different days. All rates were measured over a 7-fold SO_2 pressure range, showing a linear correlation with the neutral density and a standard deviation <15%. Nevertheless, a conservative error of 30% was given, due to the uncertainties of the neutral pressure measurements. The reaction efficiencies were expressed as the ratio of the bimolecular rate constants *k* to the collision rates that were calculated according to the average dipole orientation (ADO) theory [61].

Collision-induced dissociation (CID) experiments were carried out with the MS^n function of the LTQ XL mass spectrometer. Helium was used as the collision gas at a pressure of ca. 3×10^{-3} Torr. Typical normalized collision energies (NCE) were in the range of 10% and 50%, depending on the isolated ion, whereas the activation time and *Q* value were set to 30 ms and 0.250, respectively.

All spectra were recorded and elaborated using the Xcalibur software (version 2.0.6, Thermo Fisher Scientific, Bremen, Germany) supplied with the instrument.

3. Results and Discussion

3.1. The $NaV_3O_9^{2-}$ and $H_2NaV_3O_{10}^{2-}$ Reactant Dianions

Trimeric species of $NaV_3O_9^{2-}$ and $H_2NaV_3O_{10}^{2-}$ general formula were generated in the gas phase by electrospraying aqueous solutions of sodium metavanadate. The speciation of this salt was deeply investigated both in solution [62,63] and in the gas phase [64–67], highlighting the formation of discrete multi-charged anions containing several vanadium atoms organized in higher structures (e.g., dimer, trimer, tetramer).

Before introducing SO_2 into the trap, both $NaV_3O_9^{2-}$ and $H_2NaV_3O_{10}^{2-}$ reactant ions were mass-*to*-charge selected and exposed to helium buffer gas over long activation times (maximum a. t. = 10 s). Since no remarkable signal loss occurred as a result of the isolation and subsequent accumulation, these doubly-charged species can be considered stable towards spontaneous dissociation in the gas phase. Hence, CID experiments were performed to obtain salient structural information that was interpreted in the light of our previous calculations on similar dianionic species [48,49]. In particular, the $NaV_3O_9^{2-}$ dianion can be associated with the analogous $HV_3O_9^{2-}$ hydroxovanadate species characterized by a V_2O_6 four-membered ring connected to a VO_3 moiety [49]. Indeed, pentavalent vanadium derivatives form polyoxovanadates showing repetitive units of VO_3 revealed at *m*/*z* 99 by mass spectrometry [67]. Accordingly, the $NaV_3O_9^{2-}$ parent ion at *m*/*z* 160 dissociates into two singly-charged fragments at *m*/*z* 221 and 99 that are respectively consistent with the anions of the general formula: $NaV_2O_6^-$ and VO_3^- (Figure 1).

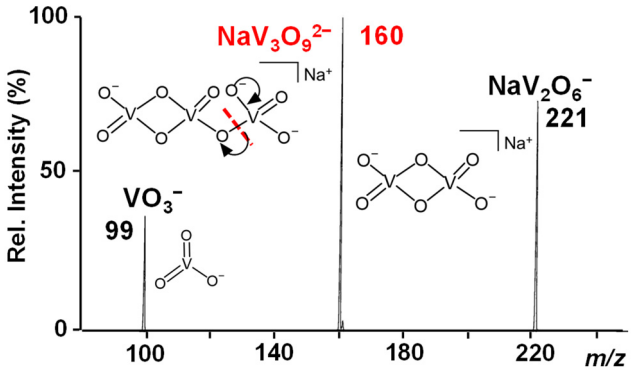

Figure 1. IT CID mass spectrum of the NaV3O9^{2-} reactant ion at m/z 160.

We can thus suppose that the VO_3 moiety is released as a consequence of a V-O cleavage induced by the collision of the parent species with the background helium gas forming a $NaV_2O_6^-$ counterpart. $NaV_2O_6^-$ maintains a V_2O_6-closed structure in agreement with the CID mass spectrum of the similar $HV_3O_9^{2-}$ species, which dissociates into VO_3^- and $HV_2O_6^-$, as theoretically described elsewhere [49].

Passing to the $H_2NaV_3O_{10}^{2-}$ ion at m/z 169, it dissociates either by breaking into two singly-charged fragments, respectively corresponding to $H_2VO_4^-$ (m/z = 117) and $NaV_2O_6^-$ (m/z = 221) anions, or by losing an H_2O molecule with the formation of the doubly-charged daughter species at m/z 160 (Figure 2a).

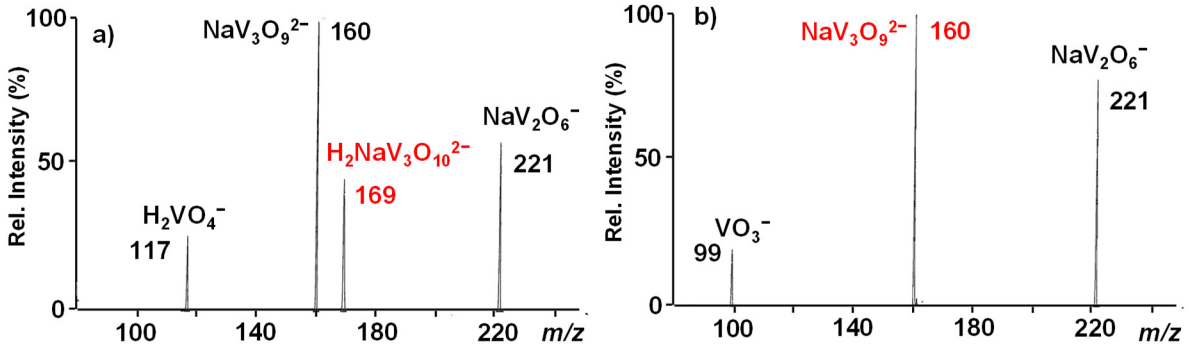

Figure 2. IT CID mass spectra of (**a**) the H2NaV3O102− reactant ion at m/z 169 and (**b**) the NaV3O9^{2-} daughter ion at m/z 160 isolated from the MS3 sequence 169→160.

The latter was, in turn, isolated through the sequence 169 → 160 and submitted to MS^3 dissociation, giving rise to the same fragmentation pattern already observed for the $NaV_3O_9^{2-}$ dianion (Figure 2b vs. Figure 1), thus pointing to the same structure.

The doubly-charged species at m/z 169 could be thus composed of a mixture of $H_2NaV_3O_{10}^{2-}$ and the isomeric hydrated electrostatic complex ion $[NaV_3O_9{\cdot}H_2O]^{2-}$. However, the loss of a water molecule forming a daughter ion with a $V_2O_6^{2-}$ four-membered ring scaffold was also observed for the covalent open-chain pirovanadate dianion, $H_2V_2O_7^{2-}$. The theoretical structure predicted for this species is characterized by two vicinal OH groups that are involved in the H_2O release resulting from a fast proton transfer reaction [48]. In addition, when exposed to H_2O in the trap, a naked $NaV_3O_9^{2-}$ dianion proved, even for the longest possible time, to be unreactive towards the addition of a water molecule.

In light of this experimental evidence and always keeping a +5 oxidation state for the vanadium atoms, we propose that the H2NaV3O10^{2-} parent ion at m/z 169, presumably formed in solution by a hydrolysis reaction at the expense of the NaV3O92− dianion, may be characterized by an open structure, showing an H2VO4 terminal moiety which is

released as the mono-anion of the vanadic acid ($H2VO^{4-}$) through an intracluster rearrangement, according to Scheme 1. The singly charged vanadate, $H2VO^{4-}$, is indeed a stable and deeply characterized species, previously obtained as a product of an ion-molecule reaction between the $H2V2O7^{2-}$ dianions and SO_2 [48].

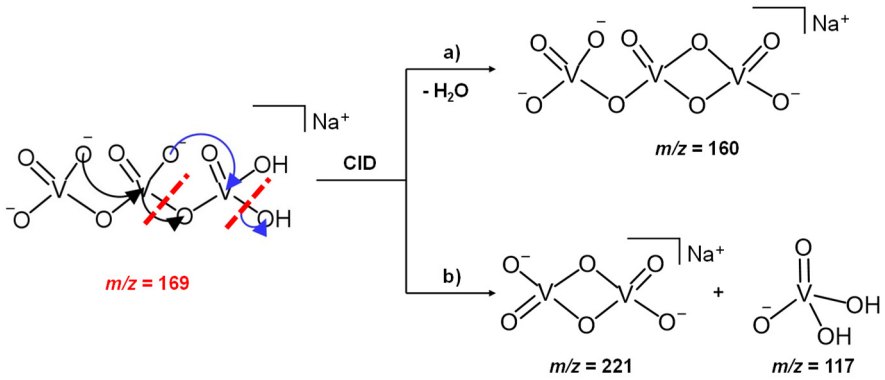

Scheme 1. CID mechanism of the $H_2NaV_3O_{10}^{2-}$ reactant ion at m/z 169.

3.2. Reactivity of $NaV_3O_9^{2-}$ and $H_2NaV_3O_{10}^{2-}$ Dianions towards SO_2

In the presence of sulphur dioxide in the ion trap, a thermal $NaV_3O_9^{2-}$ dianion binds an SO_2 molecule, giving the ligated $[NaV_3O_9{\cdot}SO_2]^{2-}$ addition product (Equation (1)). It in turn reacts with a second SO_2, forming two singly-charged product ions according to Equation (2).

$$NaV_3O_9^{2-} + SO_2 \rightarrow [NaV_3O_9{\cdot}SO_2]^{2-} \quad (1)$$

$$[NaV_3O_9{\cdot}SO_2]^{2-} + SO_2 \rightarrow [NaV_2O_6{\cdot}SO_2]^{-} + VO_3SO_2^{-} \quad (2)$$

The reaction sequence was confirmed by the kinetic analysis reported in Figure 3 showing both the reactivity of the $NaV_3O_9^{2-}$ parent ion (Figure 3a) and that of its ligated product, $[NaV_3O_9{\cdot}SO_2]^{2-}$, obtained by the direct addition of the first SO_2 molecule (Figure 3b).

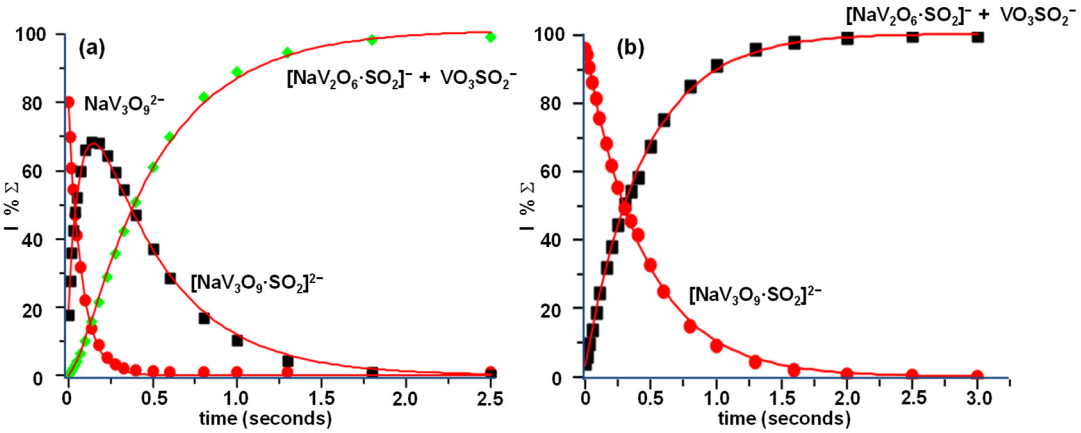

Figure 3. Kinetic plot and best fit lines of the reactions of thermal (**a**) $NaV_3O_9^{2-}$ ions with SO_2, $P(SO_2) = 2.1 \times 10^{-7}$ torr, R^2 ($NaV_3O_9^{2-}$) = 0.9991, R^2 ($NaV_3O_9{\cdot}SO_2^{2-}$) = 0.9980, R^2 ($NaV_2O_6{\cdot}SO_2^{-}$ + $VO_3SO_2^{-}$) = 0.9992 and (**b**) $[NaV_3O_9{\cdot}SO_2]^{2-}$ ions with SO_2 $P(SO_2) = 2.2 \times 10^{-7}$ torr, R^2 ($NaV_3O_9{\cdot}SO_2^{2-}$) = 0.9997, R^2 ($NaV_2O_6{\cdot}SO_2^{-}$ + $VO_3SO_2^{-}$) = 0.9989.

The rate constants of the two reactions at 298 K, as measured from the kinetic plots, amount to $k_1 = 1.40 \times 10^{-9}$ and $k_2 = 0.39 \times 10^{-9}$ ($\pm$30%) $cm^3\ s^{-1}\ molec^{-1}$, whereas the reactions' efficiencies are estimated to be slightly > 100% and 34.5%, respectively.

A possible reaction mechanism can be postulated based on the borderline acid nature of the SO_2 neutral reagent and on the heteronuclear four-membered stable structure pre-

dicted for the $VO_3SO_2^-$ product ion [48]. According to Scheme 2, in fact, after the addition of an SO_2 molecule, the attack of the second SO_2 to the opposite side of the dianionic species triggers the breaking of a V-O bond containing a bridged oxygen atom and the formation of new V-O and S-O bonds, eventually leading to two singly charged products, $[NaV_2O_6{\cdot}SO_2]^-$ and $VO_3SO_2^-$. Hence, two SO_2 molecules are needed to activate the bond-forming reaction, one of which only plays a spectator role, remaining non-covalently attached to the $NaV_2O_6^-$ anion and forming the $[NaV_2O_6{\cdot}SO_2]^-$ product ion. In support of this hypothesis, an analogous $[HV_2O_6{\cdot}SO_2]^-$ electrostatic structure was predicted for the product of the reaction of $V_2O_6^{2-}$ with SO_2 and H_2O [49].

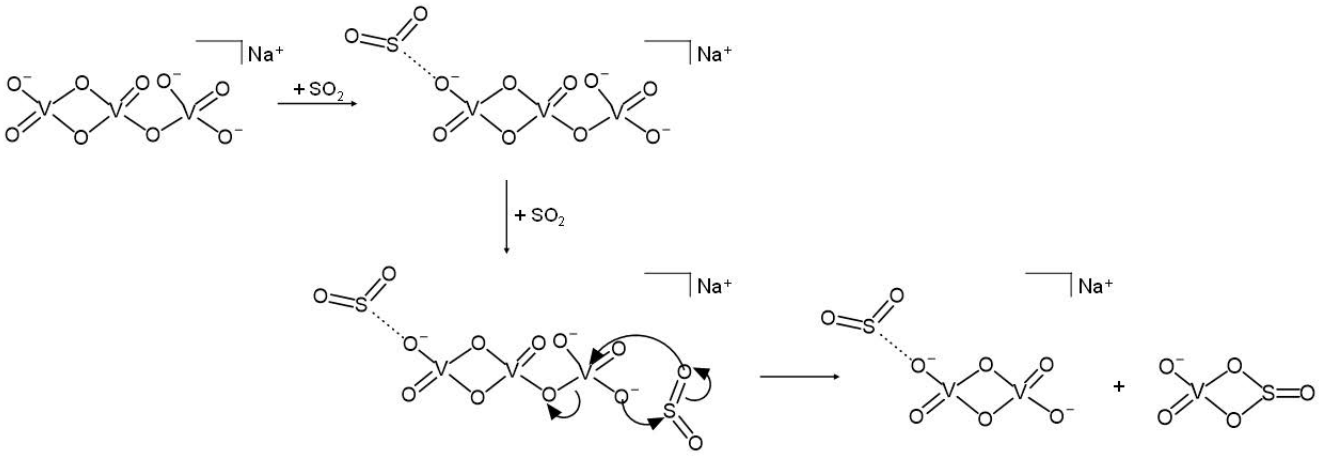

Scheme 2. Plausible reaction mechanism of $NaV_3O_9^{2-}$ ions with SO_2 based on the corresponding kinetic plot.

When moving on to the reactivity of the $H_2NaV_3O_{10}^{2-}$ dianionic species to sulphur dioxide, two parallel reaction channels were highlighted: an OH anion transfer to SO_2 leading to $HOSO_2^-$ and $HNaV_3O_9^-$ product ions (Equation (3a)), and a V-O cleavage process assisted by the SO_2 molecule (Equation (3b)), forming $[NaV_2O_6{\cdot}SO_2]^-$ and the $H_2VO_4^-$ vanadate anion.

$$H_2NaV_3O_{10}^{2-} + SO_2 \rightarrow HOSO_2^- + HNaV_3O_9^- \quad (3a)$$

$$H_2NaV_3O_{10}^{2-} + SO_2 \rightarrow [NaV_2O_6{\cdot}SO_2]^- + H_2VO_4^- \quad (3b)$$

As shown in the kinetic plot of Figure 4, the whole process is fast and efficient, showing a $k_3 = 1.15 \times 10^{-9}$ ($\pm$30%) $cm^3\ s^{-1}\ molec^{-1}$ and an efficiency of 100%. The OH^- transfer (Equation (3a)) predominates over the V-O cleavage, as demonstrated by the branching ratio between the two reaction channels (Equation (3a) vs. Equation (3b)), amounting to 3.7. The high rate constant of reaction 3.1, very close to that observed for a similar system [48], seems to confirm our previous experimental evidence of a hydroxide structure for the $H_2NaV_3O_{10}^{2-}$ dianion, rather than a hydrated one. Hydrolysis reactions, in fact, occur at a much slower rate [49].

Interestingly, reaction 3 is a regioselective process, the outcome of which depends on where the SO_2 molecule approaches the $H_2NaV_3O_{10}^{2-}$ dianion (Scheme 3). If sulphur dioxide coordinates the O-H bond, then pathway (a) of Scheme 3 takes place (Equation (3a)). Hence, the $H_2NaV_3O_{10}^{2-}$ parent ion behaves as an effective HO^- donor, forming the bisulfite ionic species $HOSO_2^-$ and a second product, $HNaV_3O_9^-$, reasonably consisting of a V_2O_6 four-membered ring connected to a VO_3 moiety, as in the case of the similar $H_2V_3O_9^-$ dianion obtained by the reaction of the $HV_3O_9^{2-}$ species with SO_2 and H_2O [49].

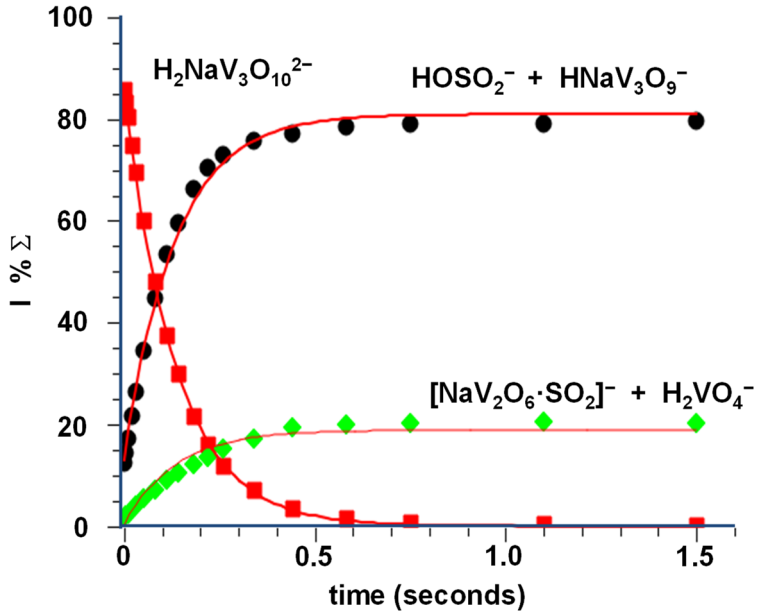

Figure 4. Kinetic plot and best fit lines of the reaction of thermal $H_2NaV_3O_{10}^{2-}$ ions with SO_2, $P(SO_2) = 2.1 \times 10^{-7}$ torr, R^2 ($H_2NaV_3O_{10}^{2-}$) = 0.9998, R^2 ($H_2VO_4^-$ + $NaV_2O_6{\cdot}SO_2^-$) = 0.9652, R^2 ($HOSO_2^-$ + $HNaV_3O_9^-$) = 0.9964.

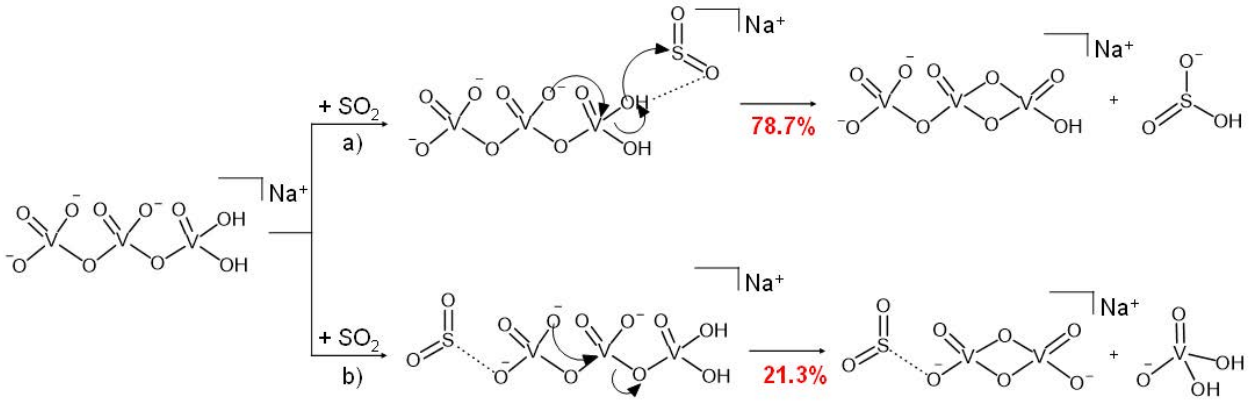

Scheme 3. Plausible reaction mechanism of $H_2NaV_3O_{10}^{2-}$ ions with SO_2 based on the corresponding kinetic plot.

Conversely, when the SO_2 molecule attacks the $H_2NaV_3O_{10}^{2-}$ dianion on the opposite side, or at least far from the –OH groups, we observe the bond-forming reaction illustrated in Scheme 3b (Equation (3b)). Accordingly, the stable V_3O_{10} kernel is broken with the formation of two singly charged products, the $H_2VO_4^-$ vanadate and the $[NaV_2O_6{\cdot}SO_2]^-$ anions, the latter being also formed in Equation (2) (Scheme 2).

The asymmetric structure of the $H_2NaV_3O_{10}^{2-}$ reactant ion may reasonably explain the occurrence of the regioselective process, as the SO_2 molecule can approach the dianion from two chemically different extremities. Similar reactions have already been observed in the gas phase, where a plethora of different factors (e.g., thermodynamic, kinetic, electronic, steric, and orbital) can act by affecting the branching ratios of alternative reaction products [68–70]. As to the reactivity of the OH terminal of $H_2NaV_3O_{10}^{2-}$, it is worth recalling that hydroxylation of acidic sites of vanadium-oxide-based materials, due to the reaction of the ubiquitous water, is known to change the electronic properties and the structure of the catalytic active sites of such materials [71].

Moreover, the open $H_2NaV_3O_{10}^{2-}$ dianion is substantially less constrained compared to the other $NaV_3O_9^{2-}$ reactant species characterized by a V_2O_6 four-membered ring. Hence, when SO_2 coordinates the $H_2NaV_3O_{10}^{2-}$ dianion from the VO_3 side, a free terminal O^- can play a nucleophilic attack on the vicinal vanadium atom, driving the formation of the two mono-charged products (Scheme 3, pathway (b)).

4. Conclusions

Fast and efficient reactions between polyvanadate dianions and sulphur dioxide have been reported in this study. Two SO_2 molecules, once sequentially added to the doubly charged vanadium oxide anion, $NaV_3O_9^{2-}$, lead to the breakage of the stable V_3O_9 kernel.

Otherwise, the hydroxide $H_2NaV_3O_{10}^{2-}$ dianion reacts with sulphur dioxide in a regioselective process by following two different pathways according to which an SO_2 molecule can promote either the breakage of a terminal V-OH bond or the V_3O_{10} kernel.

All these reactions are associated with charge separation processes that result in two singly charged product ions by the formation of new V-O and S-O bonds. The charge separation occurs exclusively as a result of the chemical reaction with sulfur dioxide, in which the dipole moment plays a crucial role in promoting the ion-neutral bonding.

Author Contributions: Conceptualization, A.T. and C.S.; methodology, A.T.; validation, A.T., F.P. and C.S.; Funding acquisition, G.d.P.; investigation, C.S.; data curation, C.S.; Supervision G.d.P.; Visualization, C.S.; writing—original draft preparation, A.T. and C.S.; writing—review and editing, A.T., C.S., F.P. and G.d.P. All authors have read and agreed to the published version of the manuscript.

Funding: This research was funded by Sapienza Rome University "Progetti di Ateneo" (Projects n. RM11816428291DFF, RM11715C81A54060, AR21916B746C06BB). C.S. thanks the Dipartimento di Chimica e Tecnologie del Farmaco, Sapienza Rome University, for a post-doc position within the project Dipartimenti di Eccellenza–L. 232/2016.

Data Availability Statement: The data presented in this study are available on request from the corresponding authors.

Conflicts of Interest: The authors declare no conflict of interest. The funders had no role in the design of the study; in the collection, analyses, or interpretation of data; in the writing of the manuscript, or in the decision to publish the results.

References

1. Weckhuysen, B.M.; Keller, D.E. Chemistry, Spectroscopy and the role of supported vanadium oxides. *Catal. Today* **2003**, *78*, 25–46. [CrossRef]
2. Chenier, J.P. *Survey of Industrial Chemistry*; John Wiley & Sons: New York, NY, USA, 1987; pp. 45–57.
3. Whittingham, M.S. Lithium batteries and cathode materials. *Chem. Rev.* **2004**, *104*, 4271–4302. [CrossRef] [PubMed]
4. Zhang, C.; Song, H.; Zhang, C.; Liu, C.; Liu, Y.; Cao, G. Interface reduction synthesis of $H_2V_2O_3$ nanobelts-graphene for high-rate Li-ion batteries. *J. Phys. Chem. C* **2015**, *119*, 11399.
5. Xu, X.; Yan, M.; Tian, X.; Yang, C.; Shi, M.; Wei, Q.; Xu, L.; Mai, L. In situ investigation of Li and Na transport with single nanowire electrochemical devices. *Nano Lett.* **2015**, *15*, 3879–3884. [CrossRef]
6. Anjass, M.; Lowe, G.A.; Streb, C. Molecular vanadium oxides for energy conversion and energy storage: Current trends and emerging opportunities. *Angew. Chem. Int. Ed.* **2021**, *60*, 7522–7532. [CrossRef]
7. Johnson, G.; Tyo, C.C.; Castleman, A.W. Cluster reactivity experiments: Employing mass spectrometry to investigate the molecular level details of catalytic oxidation reactions. *Proc. Natl. Acad. Sci. USA* **2008**, *105*, 18108–18113. [CrossRef]
8. Johnson, G.E.; Mitrić, R.; Bonačić-Koutecký, V.; Castleman, A. Clusters as model systems for investigating nanoscale oxidation catalysis. *Chem. Phys. Lett.* **2009**, *475*, 1–9. [CrossRef]
9. Schlangen, M.; Schwarz, H. Effects of ligands, cluster size, and charge state in gas-phase catalysis: A happy marriage of experimental and computational studies. *Catal. Lett.* **2012**, *142*, 1265–1278. [CrossRef]
10. Dietl, D.-C.N.; Troiani, A.; Schlangen, M.; Ursini, O.; Angelini, G.; Apeloig, Y.; de Petris, G.; Schwarz, H. Mechanistic aspects of gas-phase hydrogen-atom transfer from methane to $[CO]^+$ and $[SiO]^+$: Why do they differ? *Chem. Eur. J.* **2013**, *19*, 6662–6669. [CrossRef]
11. Schlangen, M.; Schwarz, H. Probing elementary steps of nickel-mediated bond activation in gas-phase reactions: Ligand- and cluster-size effects. *J. Catal.* **2011**, *284*, 126–137. [CrossRef]
12. Vikse, K.L.; McIndoe, J.S. Mechanistic insights from mass spectrometry: Examination of the elementary steps of catalytic reactions in the gas phase. *Pure Appl. Chem.* **2015**, *87*, 361–377. [CrossRef]

13. Vikse, K.L.; Ahmadi, Z.; McIndoe, J.S. The application of electrospray ionization mass spectrometry to homogeneous catalysis. *Coord. Chem. Rev.* **2014**, *279*, 96–114. [CrossRef]
14. Bell, R.C.; Zemski, K.A.; Kerns, K.P.; Deng, H.T.; Castleman, A.W. Reactivities and collision-induced dissociation of Vanadium oxide clusters cations. *J. Phys. Chem. A* **1998**, *102*, 1733–1742. [CrossRef]
15. Zemski, K.A.; Justes, D.R.; Castleman, A.W. Reactions of group V transition metal oxide cluster ions with ethane and ethylene. *J. Phys. Chem. A* **2001**, *105*, 10237–10245. [CrossRef]
16. Feyel, S.; Schröder, D.; Rozanska, X.; Sauer, J.; Schwarz, H. Gas-phase oxidation of propane and 1-butene with $[V_3O_7]^+$: Experiment and theory in concert. *Angew. Chem. Int. Ed.* **2006**, *45*, 4677–4681. [CrossRef] [PubMed]
17. Feyel, S.; Döbler, J.; Schröder, D.; Sauer, J.; Schwarz, H. Thermal activation of methane by tetranuclear $[V_4O_{10}]^+$. *Angew. Chem. Int. Ed.* **2006**, *45*, 4681–4685. [CrossRef] [PubMed]
18. Dietl, N.; Engeser, M.; Schwarz, H. Competitive hydrogen-atom abstraction versus oxygen-atom and electron transfers in gas-phase reactions of $[X_4O_{10}]^+$ (X = P, V) with C_2H_4. *Chem. Eur. J.* **2010**, *16*, 4452–4456. [CrossRef]
19. Zhou, S.; Li, J.; Schlangen, M.; Schwarz, H. Differences and commonalities in the gas-phase reactions of closed-shell metal dioxide clusters $[MO_2]^+$ (M = V, Nb, and Ta) with methane. *Chem. Eur. J.* **2016**, *22*, 7225–7228. [CrossRef]
20. Wang, Z.-C.; Wu, X.N.; Zhao, Y.X.; Ma, J.B.; Ding, X.L.; He, S.G. Room-temperature methane activation by a bimetallic oxide cluster $AlVO_4^+$. *Chem. Phys. Lett.* **2010**, *489*, 25–29. [CrossRef]
21. Dietl, N.; Hockendorf, R.F.; Schlangen, M.; Lerch, M.; Beyer, M.K.; Schwarz, H. Generation, reactivity towards hydrocarbons, and electronic structure of heteronuclear vanadium phosphorous oxygen cluster ions. *Angew. Chem. Int. Ed.* **2011**, *50*, 1430–1434. [CrossRef]
22. Wang, Z.-C.; Liu, J.-W.; Schlangen, M.; Weiske, T.; Schröder, D.; Sauer, J.; Schwarz, H. Thermal methane activation by a binary V-Nb transition-metal oxide cluster cation: A further example for the crucial role of oxygen-centered radical. *Chem. Eur. J.* **2013**, *19*, 11496–11501. [CrossRef] [PubMed]
23. Dietl, N.; Wende, T.; Chen, K.; Jiang, L.; Schlangen, M.; Zhang, X.; Asmis, K.R.; Schwarz, H. Structure and chemistry of the heteronuclear oxo-cluster $[VPO_4]^{\cdot+}$: A model system for the gas-phase oxidation of small hydrocarbons. *J. Am. Chem. Soc.* **2013**, *135*, 3711–3721. [CrossRef] [PubMed]
24. Li, Z.Y.; Li, H.F.; Zhao, Y.X.; He, S.G. Gold(III) mediated activation and transformation of methane on Au_1-doped vanadium oxide cluster cations $AuV_2O_6^+$. *J. Am. Chem. Soc.* **2016**, *138*, 9437–9443. [CrossRef]
25. Bell, R.C.; Castleman, A.W. Reactions of vanadium oxide cluster ions with 1,3-butadiene and isomers of butene. *J. Phys. Chem. A* **2002**, *106*, 9893–9899. [CrossRef]
26. Li, X.-N.; Xu, B.; Ding, X.-L.; He, S.-G. Interaction of vanadium oxide cluster anions with water: An experimental and theoretical study on the reactivity and mechanism. *Dalton Trans.* **2012**, *41*, 5562–5570. [CrossRef] [PubMed]
27. Li, S.; Mirabal, A.; Demuth, J.; Wöste, L.; Siebert, T. A complete reactant-product analysis of the oxygen transfer reaction in $[V_4O_{11}{\cdot}C_3H_6]^-$: A cluster complex for modelling surface activation and reactivity. *J. Am. Chem. Soc.* **2008**, *130*, 16832–16833. [CrossRef]
28. Zhao, Y.-X.; Wu, X.-N.; Ma, J.-B.; He, S.-G.; Ding, X.-L. Experimental and theoretical study of the reactions between vanadium-silicon heteronuclear oxide cluster anions with *n*-butane. *J. Phys. Chem. C* **2010**, *114*, 12271–12279. [CrossRef]
29. Janssens, E.; Lang, S.M.; Brümmer, M.; Niedziela, A.; Santambrogio, G.; Asmis, K.R.; Sauer, J. Kinetic study of the reaction of vanadium and vanadium-titanium oxide cluster anions with SO_2. *Phys. Chem. Chem. Phys.* **2012**, *14*, 14344–14353. [CrossRef]
30. Dinca, A.; Davis, T.P.; Fisher, K.J.; Smith, D.R.; Willett, G.D. Vanadium oxide anion cluster reactions with methyl isobutyrate and methyl methacrylate monomer and dimer: A study by FT/ICR mass spectrometry. *Int. J. Mass Spectrom.* **1999**, *182–183*, 73–84. [CrossRef]
31. Yuan, Z.; Li, Z.-Y.; Zhou, Z.-X.; Liu, Q.-Y.; He, S.-G. Thermal reactions of $(V_2O_5)_nO^-$ (n = 1–3) cluster anions with ethylene and propylene: Oxygen atom transfer versus molecular association. *J. Phys. Chem. C* **2014**, *118*, 14967–14976. [CrossRef]
32. Jakubikova, E.; Bernestein, E.R. Reactions of sulfur dioxide with neutral vanadium oxide clusters in the gas phase. I. Density functional theory study. *J. Phys. Chem. A* **2007**, *111*, 13339–13346. [CrossRef] [PubMed]
33. He, S.-G.; Xie, Y.; Dong, F.; Heinbuch, S.; Jakubikova, E.; Rocca, J.J.; Bernstein, E.R. Reactions of sulfur dioxide with neutral vanadium oxide clusters in the gas phase. II. Experimental study employing single-photon ionization. *J. Phys. Chem. A* **2008**, *112*, 11067–11077. [CrossRef] [PubMed]
34. Coelho, F.; Eberlin, M.N. The bridge connecting gas-phase and solution chemistries. *Angew. Chem. Int. Ed.* **2011**, *50*, 5261–5263. [CrossRef] [PubMed]
35. Schröder, D.; Engeser, M.; Schwarz, H.; Harvey, J.N. Energetics of the ligated vanadium dications VO^{2+}, VOH^{2+}, and $[V,O,H_2]^{2+}$. *ChemPhysChem* **2002**, *3*, 584–591. [CrossRef]
36. Warzok, U.; Mahnke, L.K.; Bensch, W. Soluble hetero-polyoxovanadates and their solution chemistry analysed by electrospray ionization mass spectrometry. *Chem. Eur. J.* **2019**, *25*, 1405–1419. [CrossRef]
37. Ranasinghe, Y.A.; MacMahon, T.J.; Freiser, B.S. Gas-phase reactions of lanthanum dication with small alkanes and the photodissociation of $LaC_2H_4^{n+}$ and $LaC_3H_6^{n+}$ (n = 1 and 2). *J. Am. Chem. Soc.* **1992**, *114*, 9112–9118. [CrossRef]
38. Petrie, S.; Javahery, G.; Wang, J.; Bohme, D.K. Derivatization of the fullerene dications C_{60}^{2+} and C_{70}^{2+} by ion-molecule reactions in the gas phase. *J. Am. Chem. Soc.* **1992**, *114*, 9177–9181. [CrossRef]

39. Price, S.D.; Manning, M.; Leone, S.R. Bond-forming reactions of gas-phase molecular dications. *J. Am. Chem. Soc.* **1994**, *116*, 8673–8680. [CrossRef]
40. Roithová, J.; Herman, Z.; Schröder, D.; Schwarz, H. Competition of proton and electron transfers in gas-phase reactions of hydrogen-containing dications CHX^{2+} (X = F, Cl, Br, I) with atoms, nonpolar and polar molecules. *Chem. Eur. J.* **2006**, *12*, 2465–2471. [CrossRef]
41. Roithová, J.; Schröder, D. Bond-forming reactions of molecular dications as a new route to polyaromatic hydrocarbons. *J. Am. Chem. Soc.* **2006**, *128*, 4208–4209. [CrossRef]
42. Roithová, J.; Žabka, J.; Herman, Z.; Thissen, R.; Schröder, D.; Schwarz, H. Reactivity of the $CHBr^{2+}$ dication toward molecular hydrogen. *J. Phys. Chem. A* **2006**, *110*, 6447–6453. [CrossRef]
43. Roithová, J.; Schröder, D. Bimolecular reactions of molecular dications: Reactivity paradigms and bond-forming processes. *Phys. Chem. Chem. Phys.* **2007**, *9*, 2341–2349. [CrossRef] [PubMed]
44. Roithová, J.; Schröder, D.; Schwarz, H. The SiF_3^{2+} dication: Chemistry counts! *Chem. Eur. J.* **2009**, *15*, 9995–9999. [CrossRef] [PubMed]
45. Blades, A.; Peschke, M.; Verkerk, U.; Kebarle, P. Rates of proton transfer from carboxylic acids to dianions, $CO_2(CH_2)_pCO_2^{2-}$, and their significance to observed negative charge states of proteins in the gas phase. *J. Phys. Chem. A* **2002**, *106*, 10037–10042. [CrossRef]
46. Flores, A.E.; Gronert, S. The gas-phase reactions of dianions with alkyl bromides: Direct identification of S_N2 and E2 products. *J. Am. Chem. Soc.* **1999**, *121*, 2627–2628. [CrossRef]
47. Gronert, S. Gas phase studies of the competition between substitution and elimination reactions. *Acc. Chem. Res.* **2003**, *36*, 848–857. [CrossRef] [PubMed]
48. Troiani, A.; Rosi, M.; Garzoli, S.; Salvitti, C.; de Petris, G. Vanadium hydroxyde cluster ions in the gas-phase: Bond-forming reactions of doubly-charged negative ions by SO_2-promoted V-O activation. *Chem. Eur. J.* **2017**, *23*, 11752–11756. [CrossRef] [PubMed]
49. Troiani, A.; Rosi, M.; Garzoli, S.; Salvitti, C.; de Petris, G. Sulphur dioxide cooperation in hydrolysis of vanadium oxide and hydroxide cluster dianions. *New J. Chem.* **2018**, *42*, 4008–4016. [CrossRef]
50. de Petris, G.; Cartoni, A.; Troiani, A.; Angelini, G.; Ursini, O. Water activation by SO_2^+ ions: An effective source of OH radicals. *PhysChemChemPhys* **2009**, *11*, 9976–9978. [CrossRef]
51. de Petris, G.; Troiani, A.; Rosi, M.; Angelini, G.; Ursini, O. Selective Activation of C-Cl and C-F Bonds by SO^+ Radical Cations: An Experimental and Computational Study. *ChemPlusChem* **2013**, *78*, 1065–1072. [CrossRef]
52. Troiani, A.; Rosi, M.; Salvitti, C.; de Petris, G. The oxidation of sulfur dioxide by single and double oxygen transfer paths. *ChemPhysChem* **2014**, *15*, 2723–2731. [CrossRef] [PubMed]
53. Troiani, A.; Salvitti, C.; de Petris, G. Gas-phase reactivity of carbonate ions with sulfur dioxide: An experimental study of cluster reactions. *J. Am. Chem. Soc. Mass Spectrom.* **2019**, *30*, 1964–1972. [CrossRef] [PubMed]
54. Troiani, A.; Rosi, M.; Garzoli, S.; Salvitti, C.; de Petris, G. Effective redox reactions by chromium oxide anions: Sulfur dioxide oxidation in the gas phase. *Int. J. Mass Spectrom.* **2019**, *436*, 18–22. [CrossRef]
55. Salvitti, C.; Rosi, M.; Pepi, F.; Troiani, A.; de Petris, G. Reactivity of transition metal dioxide anions MO_2^- (M = Co, Ni, Cu, Zn) with sulfur dioxide in the gas phase: An experimental and theoretical study. *Chem. Phys. Lett.* **2021**, *776*, 138555. [CrossRef]
56. Salvitti, C.; Pepi, F.; Troiani, A.; de Petris, G. Intracluster sulphur dioxide oxidation by sodium chlorite anions: A mass spectrometric study. *Molecules* **2021**, *26*, 7114. [CrossRef] [PubMed]
57. Troiani, A.; Rosi, M.; Garzoli, S.; Salvitti, C.; de Petris, G. Iron-Promoted C-C Bond Formation in the Gas Phase. *Angew. Chem. Int. Ed.* **2015**, *54*, 14359–14362. [CrossRef] [PubMed]
58. Leavitt, C.M.; Bryantsev, V.S.; de Jong, W.A.; Diallo, M.S.; Goddard, W.A., III; Groenewold, G.S.; Van Stipdonk, M.J. Addition of H_2O and O_2 to acetone and dimethylsulfoxide ligated Uranyl(V) dioxocations. *J. Phys. Chem. A* **2009**, *113*, 2350–2358. [CrossRef]
59. Bartmess, J.E.; Georgiadis, R.M. Empirical methods for determination of ionization gauge relative sensitivities for different gases. *Vacuum* **1983**, *33*, 149. [CrossRef]
60. Kuzmic, P. Program DYNAFIT for the analysis of enzyme kinetic data: Application to HIV proteinase. *Anal. Biochem.* **1996**, *237*, 260–273. [CrossRef]
61. Bowers, M.T.; Su, T. *Interactions between Ions and Molecules*; Plenum Press: New York, NY, USA, 1975.
62. Habayeb, M.A.; Hileman, O.E., Jr. 51V- FT-nmr investigations of metavanadate ions in aqueous solutions. *Can. J. Chem.* **1980**, *58*, 2255–2261. [CrossRef]
63. Aureliano, M.; Cran, D.C. Decavanadate ($V_{10}O_{28}^{6-}$) and oxovanadates: Oxometalates with many biological activities. *J. Inorg. Biochem.* **2009**, *103*, 536–546. [CrossRef] [PubMed]
64. Walanda, D.K.; Burns, R.C.; Lawrance, G.A.; Von Nagy-Felsobuki, E.I. New isopolyoxovanadate ions identified by electrospray mass spectrometry. *Inorg. Chem. Commun.* **1999**, *2*, 487–489. [CrossRef]
65. Walanda, D.K.; Burns, R.C.; Lawrance, G.A.; Von Nagy-Felsobuki, E.I. Unknown isopolyoxovanadate species detected by electrospray mass spectrometry. *Inorg. Chim. Acta* **2000**, *305*, 118–126. [CrossRef]
66. Al Hasan, N.M.; Johnson, G.E.; Laskin, J. Gas-phase synthesis of singly and multiply charged polyoxovanadate anions employing electrospray ionization and collision induced dissociation. *J. Am. Soc. Mass Spectrom.* **2013**, *24*, 1385–1395. [CrossRef] [PubMed]

67. Mutlu, E.; Cristy, T.; Graves, S.W.; Hooth, M.J.; Waidyanatha, S. Characterization of aqueous formulations of tetra- and pentavalent forms of vanadium in support of test article selection in toxicology studies. *Environ. Sci. Pollut. Res.* **2017**, *24*, 405–416. [CrossRef]
68. O'Hair, R.A.J.; Freitas, M.A.; Gronert, S.; Schmidt, J.A.R.; Williams, T.D. Concerning the regioselectivity of gas phase reactions of glycine with electrophiles. The cases of the dimethylchlorinium ion and the methoxymethal cation. *J. Org. Chem.* **1995**, *60*, 1990–1998. [CrossRef]
69. Van der Wel, H.; Nibbering, N.M.M. A gas phase study of the regioselective BH_4^- reduction of some 2-substituted maleic anhydrides. *Can. J. Chem.* **1998**, *66*, 2587–2594.
70. Wernik, M.; Hartmann, P.E.; Sipos, G.; Darvas, F.; Boese, A.D.; Dallinger, D.; Kappe, C.O. On the regioselectivity of the Gould-Jacobs reaction: Gas-phase versus solution-phase thermolysis. *Eur. J. Org. Chem.* **2020**, *2020*, 7051–7061. [CrossRef]
71. Avdeed, V.I.; Tapilin, V.M. Water effect on the electronic structure of active sites of supported Vanadium oxide catalyst $VO_x/TiO_2(001)$. *J. Phys. Chem. C* **2010**, *114*, 3609–3613. [CrossRef]